journal

J. Am. Ceram. Soc., **89** [1] 258–265 (2006)
DOI: 10.1111/j.1551-2916.2005.00678.x
© 2005 The American Ceramic Society

Characterization of First-Stage Silicon Nitride Components After Exposure to an Industrial Gas Turbine

H.-T. Lin,*,† M. K. Ferber,* and P. F. Becher*

Metals and Ceramics Division, Oak Ridge National Laboratory, Oak Ridge, Tennessee 37831-6068

J. R. Price, M. van Roode, J. B. Kimmel, and O. D. Jimenez

Solar Turbines Incorporated, San Diego, California 92101

This paper provides a summary of recent efforts undertaken to examine the mechanical properties and microstructural stability of first-stage silicon nitride blades and nozzles after field testing in an industrial gas turbine. Two commercially available silicon nitrides, i.e., Kyocera SN282 vanes and SN281 blades, were successfully evaluated in the 100 h final phase engine test at Solar Turbines Incorporated. The turbine rotor inlet temperature was increased from 1010° to 1121°C at 100% speed during the engine test with efficiency increasing from 28.8% to 30.1%. Results of scanning electron microscopy showed that apparent materials recession still occurred during the 100 h engine test, especially in the leading and trailing edge regions where the gas pressure or velocity was the highest. The apparent material recession of the airfoils resulted from the volatilization of the normally protective silica layer, evidenced by the increased surface roughness and porous $Lu_2Si_2O_7$ surface layer features. On the other hand, mechanical results generated using a ball-on-ring test technique showed that little strength degradation was measured after the 100 h engine test.

I. Introduction

In 1992 the Ceramic Stationary Gas Turbine (CSGT) Program was initiated by the U.S. Department of Energy (DOE). The program objectives were to improve fuel efficiency and output power and reduce NO_x and CO emissions in land-based gas turbines by replacement of cooled metallic first-stage blades and nozzles and the combustor liner with uncooled advanced ceramic components. The CSGT initiative was motivated by a DOE-sponsored feasibility study by Battelle Memorial Institute (Columbus, OH), which showed that significant energy gains and emission reductions could be achieved by the insertion of advanced ceramics into the hot sections of existing gas turbine engines in the United States, particularly in those engines for power-and-steam cogeneration.[1,2] In September 1992 Solar Turbines Incorporated (Solar) was awarded CSGT program funding to gain experience in the design and implementation of ceramic components, and also to increase the experience base on issues regarding the behavior of ceramic components in land-based gas turbine environments.[3,4] The engine selected for retrofitting ceramic components was Solar's Centaur 50S (San Diego, CA), which has a nominal 4 MW electrical output.

High-performance advanced Si_3N_4 and SiC ceramics were considered the leading candidates for first-stage blades and nozzles because of their excellent high-temperature thermomechanical performance and corrosion and oxidation resistance compared with their metallic counterparts.[5,6] Commercially available AS800 (from Honeywell Ceramic Components, Torrance, CA) and SN88 (from NGK Insulators Ltd., Nagoya, Japan) silicon nitrides were the candidate materials selected for blade and nozzle applications, respectively, based on extensive mechanical testing and probabilistic component life prediction efforts.[7,8]

The first CSGT field test with 62 AS800 first-stage blades and SiC–SiC ceramic matrix composite (CMC) combustor liners was initiated in May 1997 at the ARCO Bakersfield enhanced oil recovery site.[9] The CSGT engine accumulated 948 h over the duration of the first field test in addition to in-house 4 h qualification testing and 100 h endurance testing, yielding a total test time of 1052 h at full load. Borescope inspections conducted after 212 and 533 h of operation revealed no apparent changes in surface appearance nor any crack generation in the CMC combustor liners and first-stage AS800 ceramic turbine blades compared with observations of these hot section parts observed after the 100 h acceptance test at Solar. However, at 948 h of full load operation, the engine experienced an emergency shutdown because of turbine underspeed. Borescope inspection revealed that this was because of catastrophic blade failure, and blade failure cause was attributed to impact damage from a metallic locating pin from the inner combustor liner.[9] A subsequent field test of AS800 blades and SiC/SiC CMC combustor liners was terminated at 352 h[10] because of second blade failure that appeared to be caused by a piece of superalloy, which had separated at a braze joint in the compressor section and impacted the AS800 blades.

A planned 100 h in-house nozzle engine test of 42 SN88 nozzles was initiated in September 1998.[11,12] The test consisted of cold and hot engine restarts and shutdown cycles that progressively increased the severity of stresses and thermal gradients on the nozzle. Borescope inspections were routinely conducted after shutdown cycles. After 68 h of cyclic engine testing, the borescope inspection showed critical cracks, which initiated in a low-temperature airfoil region of several nozzle airfoils, and the test was therefore discontinued. Analyses of the cracked nozzles by scanning electron microscopy (SEM) and X-ray diffraction revealed changes in microstructure in the secondary phase, which were attributed to the combustion environment. Dynamic fatigue tests at Oak Ridge National Laboratory (ORNL) on as-received SN88 at 850°C in air suggested that changes in the secondary phase (from $Yb_4Si_2O_7N_2$ to $Yb_2Si_2O_7$ plus Yb_2SiO_5) could have resulted in the formation of an extensive damage zone. These phase changes involved material volume increases that generated large residual tensile stress in the surface region and ultimately led to the failure of the SN88 turbine nozzles.[13,14]

In April 2001 the final 100 h engine test for the CSGT Program was conducted at Solar with all three types of ceramic components, consisting of SN281 blades, SN282 nozzles, and an SiC–SiC CMC combustor liner.[8] The final total test duration

S. M. Wiederhorn—contributing editor

Manuscript No. 20591. Received May 23, 2005; approved July 18, 2005.
This work was supported by US DOE, Office of Distributed Energy, Microturbine Materials Program, under Contract DE-AC05-00OR22725 with UT-Battelle, LLC.
*Member, American Ceramic Society.
†Author to whom correspondence should be addressed. e-mail: linh@ornl.gov

was, in fact, 104 h, most of which were at the baseline turbine rotor inlet temperature (TRIT) of 1010°C. However, the engine was also operated for short times (<1 h) at TRITs of 1066° and 1121°C. Visual inspection after completion of engine testing revealed no apparent damage (i.e., cracks) nor any surface changes in any of the components. Note that the hottest steady-state temperature on the first-stage nozzles and blades is 1288° and 1121°C, respectively. These first-stage components experienced two emergency shutdowns from full load because of the failure in power output system, and the temperature of these first-stage components reached ~150°C in about 45 min. The estimated pressure at the first-stage component chamber was 10 atm, and the gas composition measured for the exhaust is 75.12% N_2–14.44% O_2–2.94% CO_2–0.90% Ar–6.60% H_2O (in vol%)[15]. This paper describes the results of component characterization efforts on SN281 blades and SN282 nozzles after the 104 h turbine exposure. The results provide an insight into the effect of combustion environment on the microstructure and composition stability of ceramic components under conditions, which cannot be accurately reproduced in a laboratory exposure test.

II. Experimental Procedures

(1) Materials

The first-stage blades and nozzles were fabricated from SN281 and SN282 silicon nitride, respectively (Kyocera Industrial Ceramics Corp., Vancouver, WA). Kyocera developed SN281 and SN282 as variants of the same basic silicon nitride in response to the stress/temperature conditions for rotating and stationary hot section components, respectively.[16] The SN281 was densified via gas pressure sintering followed by hot isostatically pressing (HIP), while SN282 was only densified via the gas pressure sintering. The HIP operation used to densify SN281 results in a fine-grained matrix structure and a substantial reduction in internal defects. As a result, SN281 has higher mechanical strength required because of the higher stresses in rotating components, which result from the contribution of centrifugal load, in addition to the gas loads and temperature gradients experienced during operation. On the other hand, because of its relative low-strength SN282 was used for stationary components, i.e., nozzles, vane rings, and transition ducts, etc. The sintering additives employed in both materials were Lu_2O_3 and SiO_2, and the crystalline phases in both as-received materials are β-Si_3N_4 and $Lu_2Si_2O_7$. The selection of these two materials for final engine testing was based on the fact that they exhibited superior creep resistance at temperatures up to 1500°C in air, compared with any other commercially available silicon nitride ceramic in the market. The excellent creep resistance was attributed to the high thermal and microstructural stability of the $Lu_2Si_2O_7$ secondary phase.[17] In addition, observation of many clean boundaries without glassy thin film has been reported, consistent with its high-temperature creep properties.[18] It is important to note that both SN281 and SN282 components were tested without the benefit of environmental barrier coatings (EBCs).

(2) Components Characterization

The first characterization method involved dimensional inspection of the nozzles and blades before and after the engine test. Selected components were dimensionally inspected with a coordinate measurement machine (CMM). Here the primary emphasis was to measure changes in the shape of the midspan slice of the airfoil before and after engine testing.

X-ray diffraction was used to identify the predominant secondary phase(s) in the airfoil before and after the 100 h engine test. For each airfoil examined, diffraction patterns were obtained for the platform surface as well as for the convex and concave sides of the airfoil. SEM was first used to examine the surfaces of the airfoils and platforms after removal of the components from the engine. Selected components were subsequently sectioned by making a longitudinal cut parallel and adjacent to the trailing edge (Fig. 1). These pieces were subsequently polished and examined with SEM to provide an insight into the effect of the turbine environment on the long-term stability of the microstructure and chemistry of the silicon nitride ceramic components.

The biaxial flexure strength[19,20] was measured for selected components using a ball-on-ring arrangement. Disk-shaped specimens were machined from both the airfoil and platform surfaces by first diamond core drilling small cylinders having a nominal diameter of 7.0 mm. Each cylinder was then machined on one face only until the thickness was 0.5 mm. In this way, one face of each specimen always consisted of the exposed surface of either the airfoil or platform. Thus during testing, the exposed surfaces were always loaded in tension.

The test fixture consisted of a 1-mm-diameter WC ball, which was mounted on a miniature load cell. The lower support ring, which was 5.0 mm in diameter, was fabricated from a high-strength polymer. The test fixture itself was mounted on a vertical stepper motor (Z stage), which was affixed to the X–Y stages for positioning in the horizontal plane. A personal computer controlled all three stages. After placing a specimen on the lower support ring, the X–Y stages were used to position the assembly directly under the upper load ball. A calibration procedure was carried out to ensure the WC ball was centered on the lower support ring prior to the testing. The Z stage was then lowered at a rate of 0.1 mm/s until the WC ball made a light contact with the specimen. The specimen was subsequently loaded to failure at a displacement rate of 0.01 mm/s. The computer monitored and recorded the displacement, load, and time. The strength, S_b, was calculated from the equation

$$S_b = 3P(1+\nu)/(4\nu t^2)[1 + 2\ln(a/b) + ((1-\nu)/(1+\nu))(1 - b^2/2a^2)(a^2/R^2)] \quad (1)$$

where P is the ultimate sustained load, a is the radius of the support ring, b is the effective radius of contact of the loading ball on the specimen, R is the specimen radius, t is the specimen thickness, and ν is Poisson's ratio. The effective area of ball contact, b, is typically calculated using the following expressions

$$b = t \quad (z > 1.724\,t) \quad (2a)$$

$$b = (1.6\,z^2 + t^2)^{1/2} - 0.675\,t \quad (z < 1.724\,t) \quad (2b)$$

$$b = 0.325\,t \quad (z \to 0) \quad (2c)$$

where z is the contact radius for elastic loading

$$z = [(3PR_b/4)(1-\nu^2)/E + (1-\nu_b^2)/E_b]^{1/3} \quad (3)$$

where R_b is the radius of the loading ball, ν_b is the Poisson's ratio, and E_b is the elastic modulus of the ball.[21] In the present study, the z/t ratio is approximately equal to 0.08. Thus, as a first approximation, b was taken as $t/3$.

III. Results and Discussion

(1) CMM Profiles

Figure 1 shows sections of the SN282 nozzle and SN281 blade assembly after the 104 h engine test. Observations of both tested SN281 blades and SN282 nozzles reveal a light-color deposit on both the inner (concave) and outer (convex) airfoil surfaces, as shown in Fig. 1 (insets), except for the inner airfoil surface of the SN281 blades. The light-color deposits were similar to those observed earlier on AS800 and SN282 vanes without protective EBC after engine testing at Rolls-Royce Allison.[22–24] Also, visual inspections showed that the light-color phase was more prominent on SN282 nozzles than on the SN281 blades. Subsequent SEM analyses of exposed airfoil surfaces revealed that this deposit on the blades and nozzles had a composition identical to that of the secondary phase of both materials, indicating

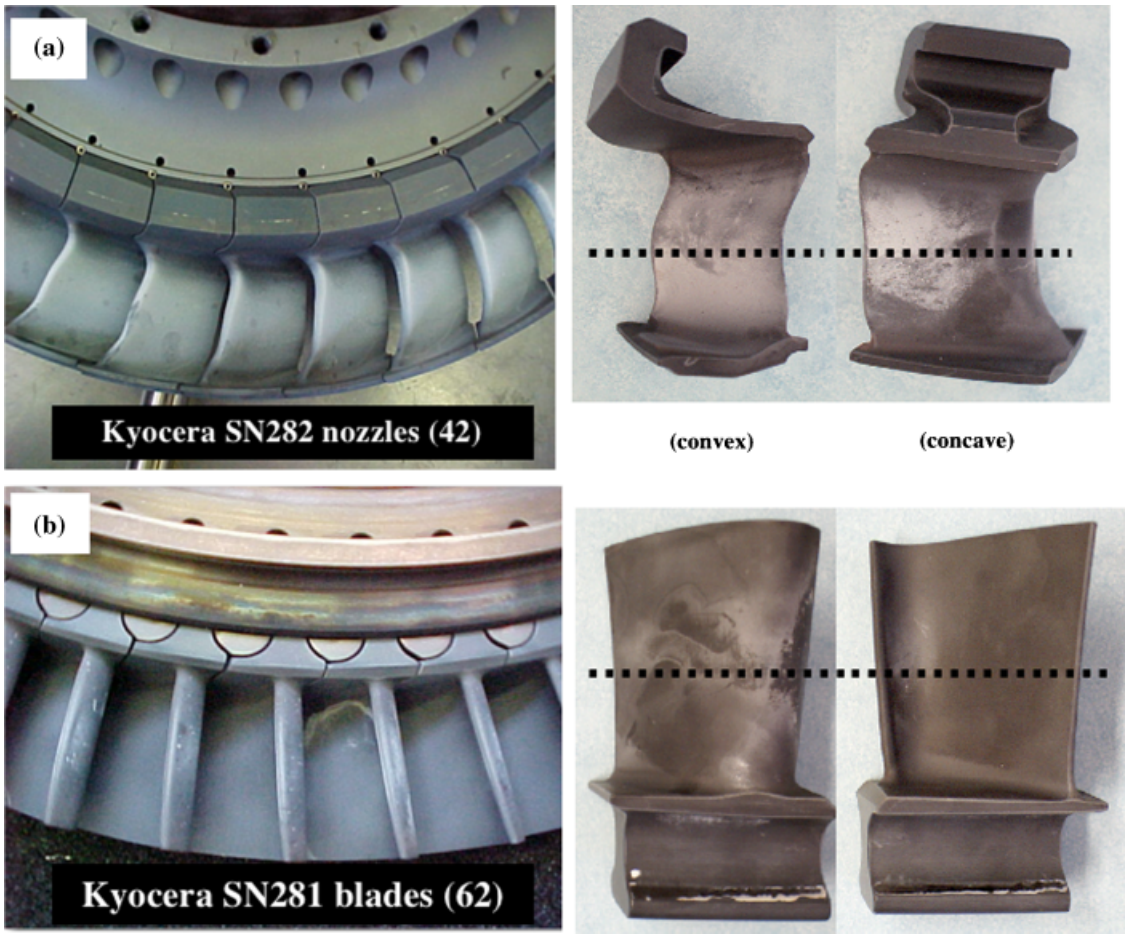

Fig. 1. Photos show the section of assembled first stage (a) SN282 nozzles and (b) SN281 blades. Photos of individual nozzle and blade after engine test are also shown for reference. The dotted lines show the airfoil region characterized in the present study.

that the silicon nitride grains had been removed as a result of material recession processes caused by oxidation reactions during exposure to high-temperature and high-pressure water vapor.[24] Subsequent X-ray analysis further confirmed that the light-color deposits on airfoil surfaces consisted of $Lu_2Si_2O_7$.

The CMM data were used to measure the airfoil profile, especially the thickness in both the leading and trailing edge regions, before and after the engine test. Results of CMM evaluation for the midspan region indicated that total line length and the integrated total surface area of the nozzles and blades after the 100 h test were similar to those measured for the as-received components, as shown in Tables I and II; any differences in these values fell within the uncertainty of the component specifications and the specific locations of each component characterized. Therefore, the CMM results suggest that little material recession occurred during the 100 h engine test. Similar results of negligible recession were also previously reported for the uncoated AS800 and SN282 vanes after <200 h of engine testing at Rolls-Royce Allison.[22,24]

(2) Microstructure Characterization

(A) First Stage SN282 Nozzles: Results of SEM examinations in the mid-span airfoil region indicated that the surface morphology developed after the 100 h engine test was a function of location with respect to the combustion gas flow (Fig. 2). For instance, at the leading edge, where the gas pressure is high and velocity was low (Fig. 2(a)), and at the trailing edge region, where the gas pressure is low and velocity is high (Fig. 2(c)), the airfoil surfaces exhibit a rough morphology with the accumulation of $Lu_2Si_2O_7$ on the surface. The hill and valley morphology corresponding to the gas flow pattern existing along the airfoil surface, which is especially prominent at the trailing edge surface (Fig. 2(c)). The presence of porous $Lu_2Si_2O_7$ surface layers resulted from the recession of silicon nitride grains as the normally protective silica scale, formed because of oxidation reaction, became unstable in the combustion environment. Thus, limited material recession has occurred, especially in both leading and trailing edge regions, even after only a 100 h engine test. On the other hand, the airfoil surface in the middle region was quite smooth with features reminiscent of an etched surface, which

Table I. Coordinate Measurement Machine (CMM) Measurements of Solar SN282 First-Stage Nozzles Before and After 100 h Engine Test

Nozzle ID	Condition	Total line length (mm)	Total surface area (mm^2)
282-44	As received	78.795	129.000
282-13	As received	78.433	127.650
282-46	100 h test	78.211	126.912
282-10	100 h test	78.782	125.953

Table II. Coordinate Measurement Machine (CMM) Measurements of Solar SN281 First-Stage Blades Before and After 100 h Engine Test

Blade ID	Condition	Total line length (mm)	Total surface area (mm^2)
281-50	As received	88.239	118.922
281-49	As received	88.518	119.387
281-107	100 h test	88.236	118.801
281-109	100 h test	88.632	118.828

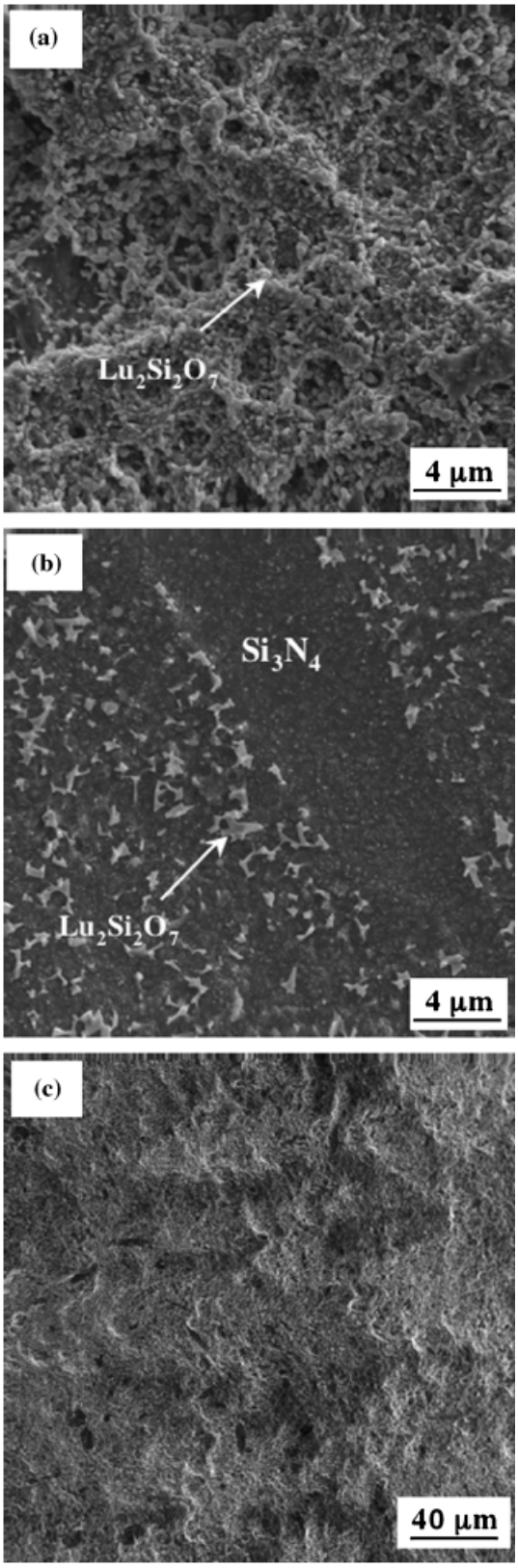

Fig. 2. Scanning electron micrographs of SN282 nozzle airfoil surface after engine test. (a) Leading nose region, (b) middle surface region, and (c) trailing edge region.

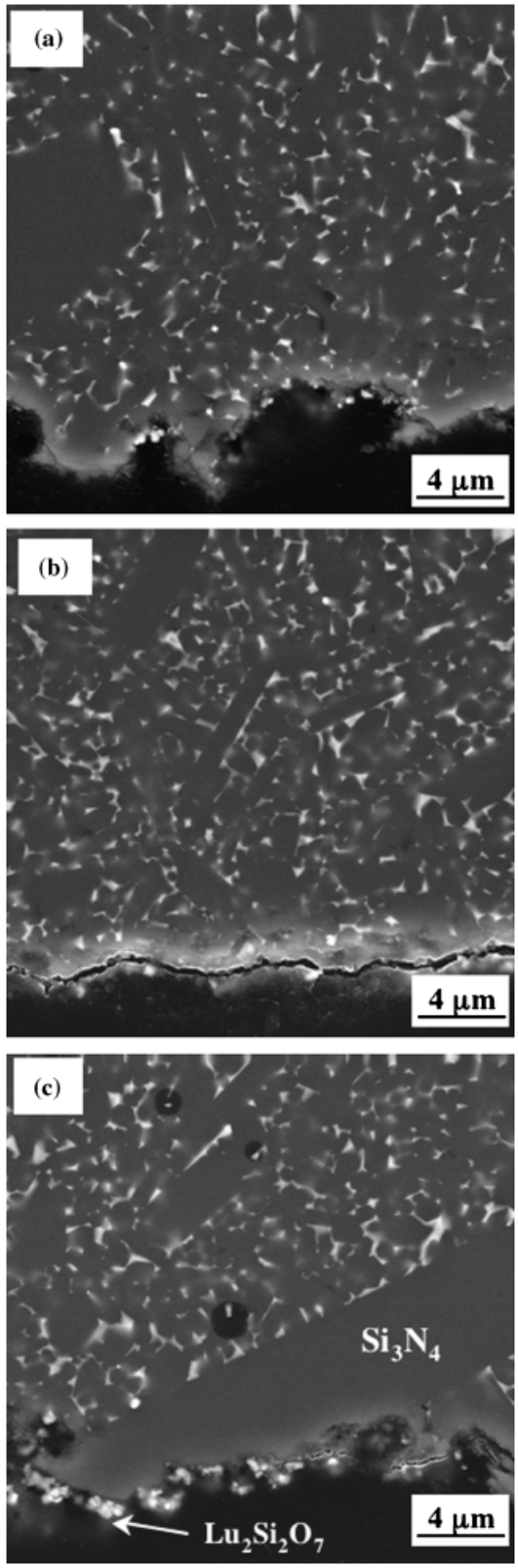

Fig. 3. Scanning electron micrographs of polished cross-section of SN282 nozzle after engine test. (a) Leading nose region, (b) middle surface region, and (c) trailing edge region.

highlighted the elongated silicon nitride grains plus $Lu_2Si_2O_7$ secondary phase (Fig. 2(b)). This reflected the moderate gas pressure and velocity pattern.

Figure 3 shows the microstructure of polished cross-sections of an SN282 nozzle corresponding to the leading, middle, and trailing edge regions. Again, both the leading edge (Fig. 3(a)) and trailing edge (Fig. 3(c)) regions began to show signs of the formation of rougher surface than that observed in the middle region (Fig. 3(b)), presumably because of the much more aggressive gas flow pattern. Also, examinations showed that there were no apparent differences in microstructure between the concave and convex sides of the SN282 nozzles. In addition, the

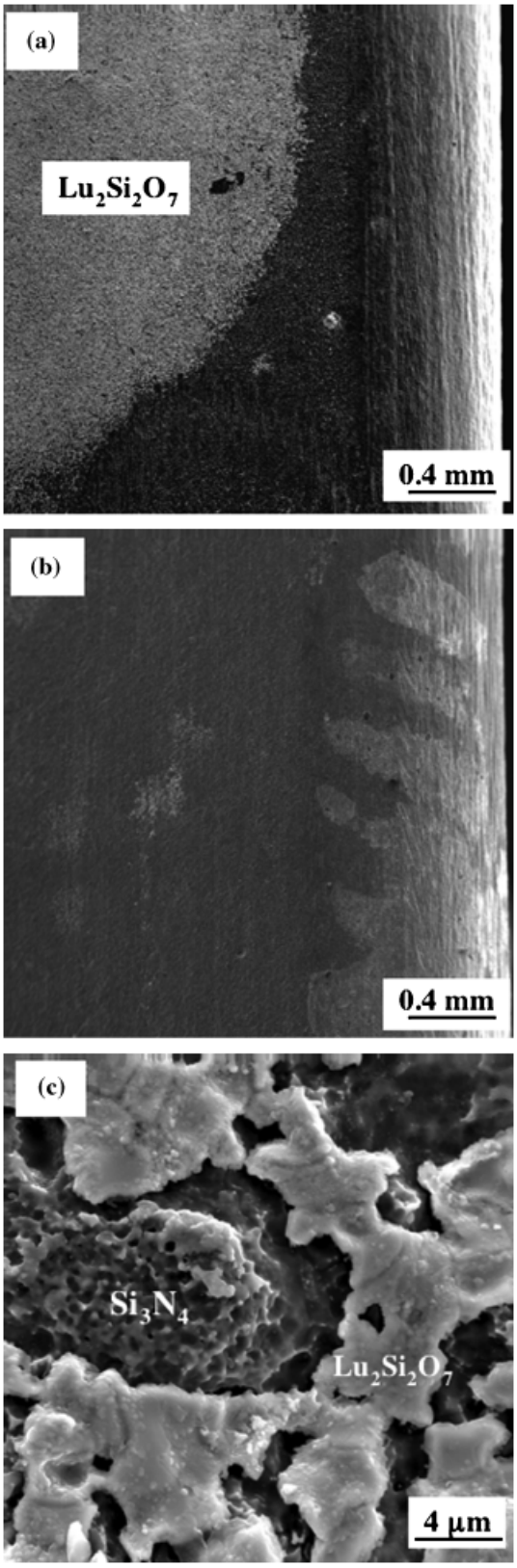

Fig. 4. Scanning electron micrographs of SN281 blade airfoil surface after engine test. (a) Convex airfoil surface region, (b) concave airfoil surface region, and (c) high magnification of convex airfoil surface where the $Lu_2Si_2O_7$ deposit was present.

SEM micrographs after engine testing illustrated the accumulation of the $Lu_2Si_2O_7$ secondary phase on the surface because of the loss of silicon nitride by environmentally induced recession. Elongated silicon nitride grains showing partial recession were also observed, but there was no change in the microstructure of the silicon nitride substrate (e.g., subsurface cracking and phase change). This material recession would be responsible for the slight increase in surface roughness after the engine test. The recession behavior of Si-based ceramics and composites in combustion environments has been well studied and reported previously.[25–28]

(B) First Stage SN281 Blades: Figure 4 shows the SEM micrographs of typical airfoil surfaces of SN281 blades after the 100 h engine test. The original machining marks in the trailing edge region were still apparent after the 100 h engine test, suggestive of little material recession. Also, observations showed that the convex surface side was always covered with a porous light-colored layer (Fig. 4(a)), which was not observed for the concave surface side (Fig. 4(b)). At higher magnification (Fig. 4(c)), the porous light-color phase exhibited a characteristic crystalline microstructure with average grain size of 3–4 μm, and was, again, identified as $Lu_2Si_2O_7$ by X-ray analysis. The source of this thin layer of porous $Lu_2Si_2O_7$ coating could come from the upstream SN282 nozzles. When the silicon nitride grains in the surface region of SN282 nozzles recessed because of oxidation and $Si(OH)_4$ formation processes, the $Lu_2Si_2O_7$ powders would be loosely bonded to the silicon nitride substrate, and would then be eroded by the high-velocity gas glow and redeposited on the convex side airfoil surfaces of the down stream SN281 blades.

The surface morphology of the SN281 blade airfoil was also a function of location with respect to the combustion gas flow, as shown in Fig. 5. The leading and trailing edge regions, which were in general not covered with a $Lu_2Si_2O_7$ deposit layer, exhibited relatively rough features because of the high impact gas pressure or gas velocity, similar to that observed for the SN282 nozzle (Figs. 2(a) and (c)). Also, in the middle region where no $Lu_2Si_2O_7$ deposit layer was present, the airfoil surface again exhibited a smooth etched feature with silicon nitride grains and $Lu_2Si_2O_7$ secondary phase, again similar to those observed for the SN282 nozzle (Fig. 2(b)). In addition, observations on the concave side (always without $Lu_2Si_2O_7$ deposit layer) revealed that the surface features developed along the mid-span airfoil were similar to those observed on the convex side.

Figure 6 shows the representative polished cross-sections of a 100 h-tested SN281 blade as a function of airfoil location. In general, the surface roughness correlated well with the observations on the blade surface morphology; the leading and trailing edge region exhibited more material recession (rougher surface feature) than the middle airfoil region because of the higher gas pressure or gas velocity. Again, there were no apparent differences in cross-section surface features between the concave and convex side. On the other hand, SEM results showed that the thin $Lu_2Si_2O_7$ deposit layer was adherent to the SN281 substrate, and there were no microstructure and chemistry changes underneath the thin $Lu_2Si_2O_7$ layer. Previous engine testing of SN282 vanes at Rolls-Royce Allison also suggested that the $Lu_2Si_2O_7$ phase was stable in gas turbine environments, and thus could be a potential candidate for an environmental barrier coating to protect silicon nitride components in gas turbine environments.[24]

(3) Mechanical Property Evaluation

The strength data of both SN282 nozzles and SN281 blades in the as-received condition and after the 100 h field test are shown in Figs. 7 and 8, respectively. Results showed that the strength of SN282 and SN281 biaxial discs, where the surfaces exposed during the 100 h engine test were the tensile surfaces, remained comparable with those obtained from discs taken from the as-sintered airfoils. There was a slight increase in data standard deviation for the 100 h exposed discs presumably, in part, arising from the increased occurrence of low-strength specimens resulting from the increased surface roughness (flaw size). The current mechanical test results were similar to those previously reported for the uncoated SN282 and AS800 vanes after engine testing at Rolls-Royce Allison.[24,29] Note that biaxial discs from nozzle

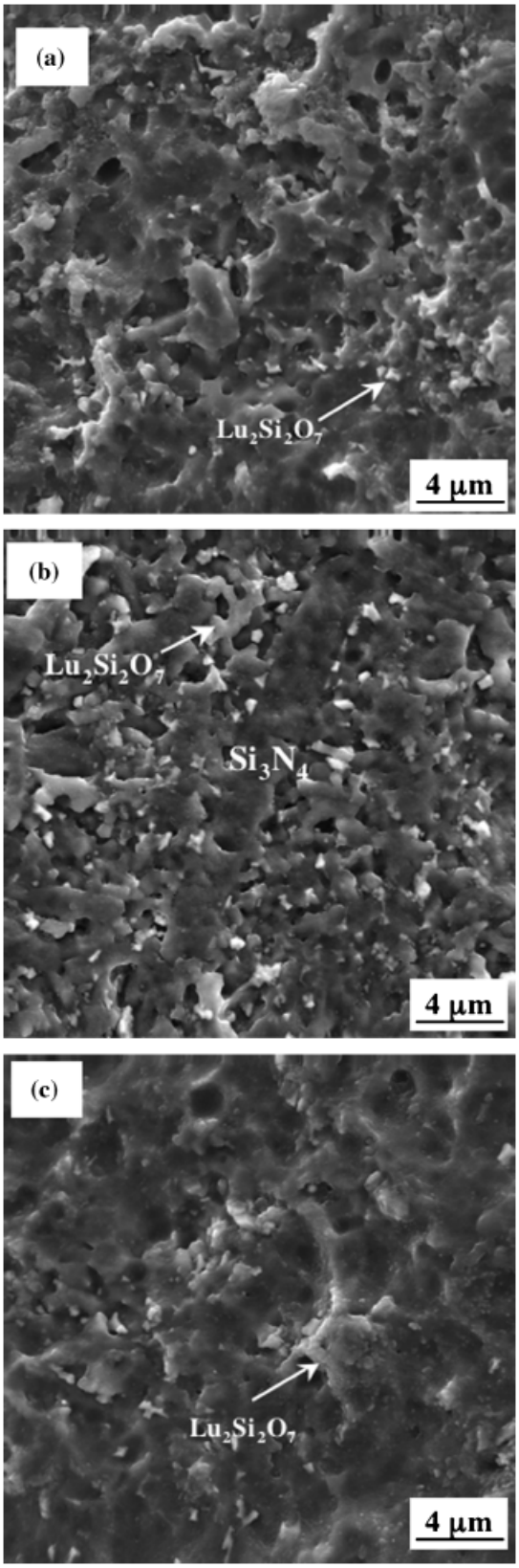

Fig. 5. Scanning electron micrographs of SN281 blade airfoil surface after engine test without $Lu_2Si_2O_7$ deposit. (a) Leading nose region, (b) middle surface region, and (c) trailing edge region.

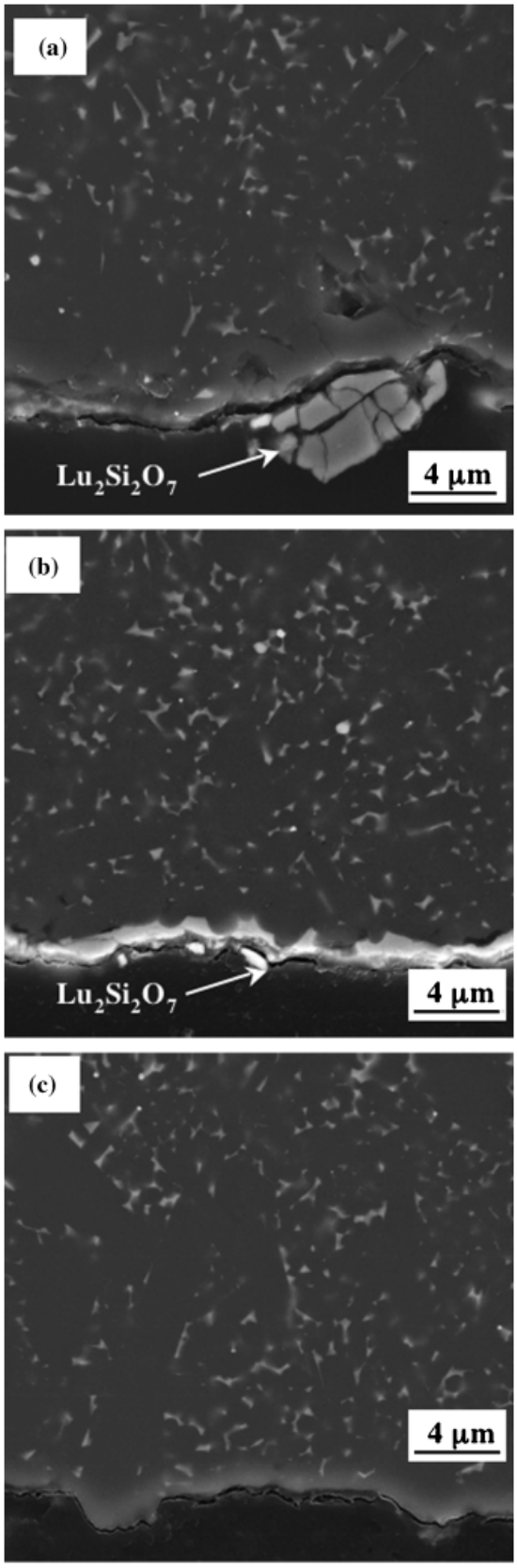

Fig. 6. Scanning electron micrographs of polished cross-section of SN281 blade after engine test. (a) Leading nose region, (b) middle surface region, and (c) trailing edge region.

shroud and blade platform regions with machined surfaces, which were only subjected to low temperatures during field tests, were also evaluated for comparison. Results showed that the strengths from the as-processed airfoil region were 25%–37% lower than those obtained from shroud and platform regions with as-machined surfaces. Similar results have been reported for silicon nitride microturbine rotors.[30] The difference in measured biaxial strength between as-processed and as-machined discs has been attributed to the differences in population and size of strength limiting flaws.[30] SEM analysis of fracture

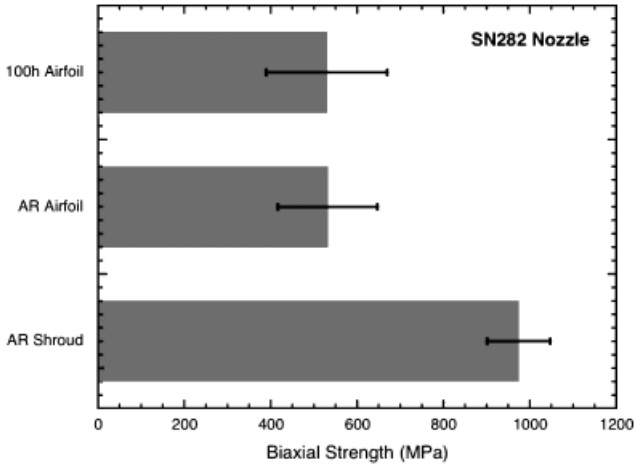

Fig. 7. Comparison of biaxial strength of discs machined from as-received (AR) shroud, AR airfoil, and 100 h tested airfoil of SN282 nozzles.

surfaces of biaxial discs from both engine-tested components (Fig. 9) showed that the fracture initiated from either clusters of large elongated silicon nitride grains or surface roughness because of recession process. For long-term application within the lifetime of gas turbine engines, the silicon nitride material recession, which would lead to dimensional instability and possible component failure, is a critical issue that needs to be addressed. Therefore, environmental protective coating systems need to be developed and engineered to protect silicon nitride components from the gas turbine environment and ensure long-term microstructure and chemical stability.

IV. Summary

SN282 nozzles and SN281 blades were successfully tested in Solar's Centaur 50S gas turbine for 100 h. Visual examinations combined with CMM data indicated no apparent large-scale damage and material recession. However, SEM examinations after engine testing showed that apparent material recession still occurred in both components, especially in the leading and trailing edge regions. The surface morphology (roughness) developed varied as a function of location and, thus, airflow pressure and velocity. The leading edge and trailing edge regions exhibited relatively rougher surfaces compared with the surface at the middle airfoil region. An adherent porous $Lu_2Si_2O_7$ layer covered the convex airfoil side of SN281 blades, possibly originating from upstream SN282 nozzles, could protect silicon nitride substrate in gas turbine environments as an EBC. Biaxial strength data showed that no mechanical degradation occurred as a result of engine testing. Also, tests of as-received components showed that discs with as-sintered surface exhibited lower strengths than those with machined surface taken from platform and shroud regions.

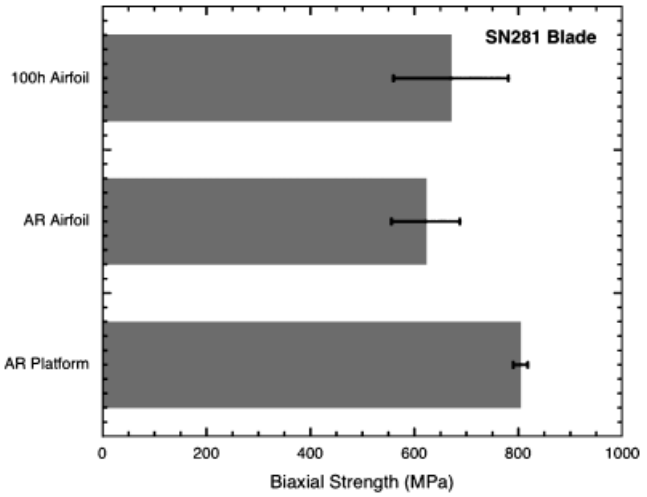

Fig. 8. Comparison of biaxial strength of discs machined from as-received (AR) platform, AR airfoil, and 100 h tested airfoil of SN281 blades.

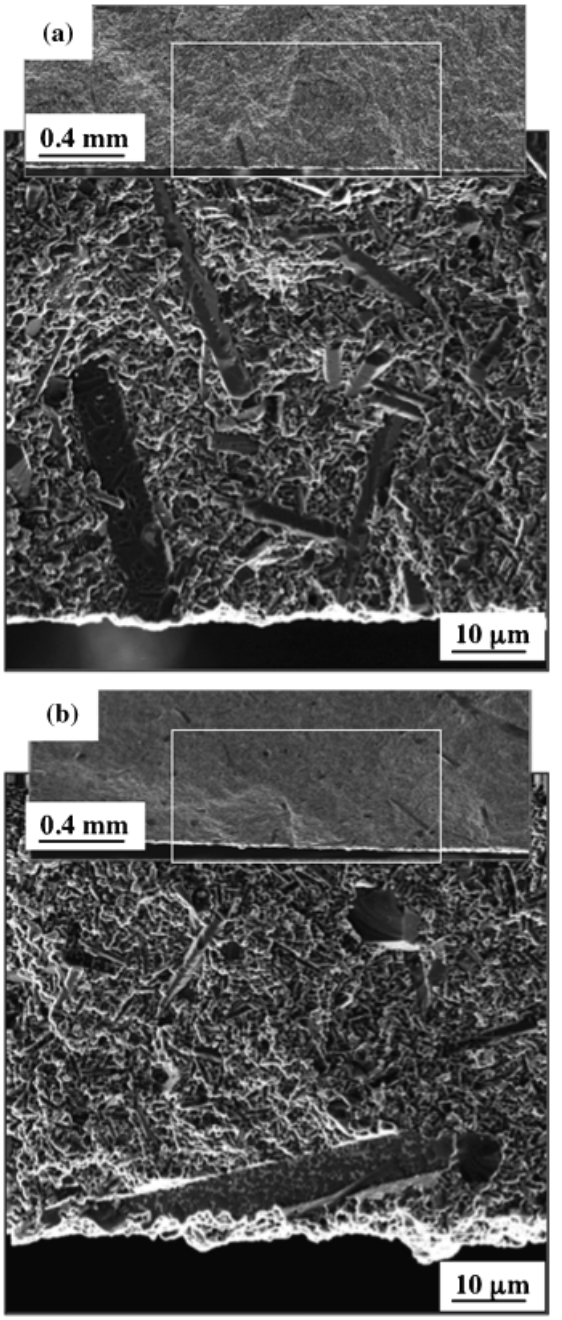

Fig. 9. Scanning electron micrographs (SEM) of fracture surfaces of biaxial disc from (a) SN282 nozzle and (b) SN281 blade. The inserted low-magnification SEM micrographs show the fracture origin of samples.

Acknowledgments

The authors thank Drs. T. N. Tiegs and P. F. Tortorelli for reviewing the manuscript.

References

[1]D. Anson, K. S. Ramesh, and M. DeCorso, "Application of Ceramics in Industrial Gas Turbines; Task 1, Technology Background"; Task 1 Report, U.S. Department of Energy Contract No. DE-AC-2-89CE40878, DOE/CE/40878-2, 1991.

[2]D. Anson, W. J. Sheppard, D. L. Norland, and M. DeCorso, "Application of Ceramics in Industrial Gas Turbines; Economics Market, Analysis, and R&D Plan"; Part 2 Report—Tasks 2, 3, and 4, U.S. Department of Energy, Contract No. DE-AC-2-89CE40878, DOE/CE/40878-2, 1991.

[3]M. van Roode, W. D. Brentnall, P. F. Norton, and G. P. Pytanowski, "Ceramic Stationary Gas Turbine Development"; ASME Paper 93-GT-309, Published in the *Proceedings of the International Gas Turbine and Aeroengine Congress and Exposition*, Cincinnati, OH, May 24–27, 1993.

[4]M. van Roode, "Ceramic Retrofit Program"; pp. 77–93 in *Proceedings of the Joint Contractors Meeting: FE/EE Advanced Turbine Systems Conference FE Fuel Cells and Coal-Fired Heat Engines Conference*, DOE/METC-93/6132, Morgantown, WV, August, 1993.

[5]D. Carruthers and L. Lindberg, "Critical Issues for Ceramics for Gas Turbines"; pp. 1258–72 in *Third International Symposium on Ceramic Components and Materials for Engines*, Edited by V. J. Tennery. American Ceramic Society, Westerville, OH, 1988.

[6]P. J. Haley, R. L. Holtman, L. E. Groseclose, S. J. Hilpisch, and A. H. Bell III, "Advanced Turbine Technology Applications Project (ATTAP)"; pp. 19–29 in *Proceedings of the Twenty-Ninth Automotive Technology Development Contractors' Coordination Meeting*. Society of Automotive Engineers, Warrendale, PA, June 1992.

[7]V. M. Parthasarathy, J. R. Price, W. D. Brentnall, G. Graves, and S. Goodrich, "Material Characterization of Candidate Silicon Based Ceramics for Stationary Gas Turbine Applications"; ASME Paper 95-GT-249, Published in the *Proceedings of the International Gas Turbine and Aeroengine Congress and Exposition*, Houston, TX, June 5–8, 1995.

[8]M. van Roode, J. R. Price, D. W. Richerson, V. Parthasarathy, and G. A. Graves, "Ceramic Stationary Gas Turbine Development—Monolithic Ceramic Component Development Summary"; ASME Paper 2001-GT-0457, Published in the *Proceedings of the 46th ASME TURBO EXPO 2001, Land, Sea, & Air*, New Orleans, LA, June 4–7, 2001.

[9]J. R. Price, O. Jimenez, L. Faulder, B. Edwards, and V. Parthasarathy, "Ceramic Stationary Gas Turbine Development—Fifth Annual Summary"; ASME Paper 98-GT-181, Published in the *Proceedings of International Gas Turbine and Aeroengine Congress and Exhibition*, Stockholm, Sweden, June 2–5, 1998.

[10]J. R. Price, O. Jimenez, V. Parthasarathy, and N. Miriyala, "Ceramic Stationary Gas Turbine Development—Sixth Annual Summary"; ASME Paper 99-GT-351, Published in the *Proceedings of the International Gas Turbine and Aeroengine Congress and Exposition*, Indianapolis, IN, June 7–10, 1999.

[11]M. van Roode, J. R. Price, S. Gates, S. Waslo, and P. Hoffman, "Ceramic Stationary Gas Turbine Development—Opportunities and Challenges"; pp. 65–72 in *Proceedings of the 7th International Gas Turbine Congress*, Vol. 1, Kobe, Japan, November 14–19, 1999..

[12]J. R. Price, O Jimenez, V. Parthasarathy, N. Miriyala, and D. Leroux, "Ceramic Stationary Gas Turbine Development Program—Seventh Annual Summary"; ASME Paper 2000-GT-0075, Published in the *Proceedings of the ASME TURBO EXPO 2000, Land, Sea, & Air*, Munich, Germany, May 8–11, 2000.

[13]H. T. Lin, M. K. Ferber, and M. van Roode, "Mechanical Reliability of Si_3N_4 Nozzles After Exposure in an Industrial Gas Turbine"; pp. 97–102 in *Proceedings of the 7th International Symposium on Ceramic Materials and Components for Engines*, Edited by J. G. Heinrich and F. Aldinger. Wiley-Vch, New York, 2001.

[14]H. T. Lin, M. K. Ferber, and T. P. Kirkland, "Evaluation of Mechanical Stability of a Commercial SN88 Silicon Nitride at Intermediate Temperatures," *J. Am. Ceram. Soc.*, **86** [7] 1176–81 (2003).

[15]O. Jimenez, H. Bagheri, J. McClain, K. Ridler, and T. Bornemisza, "CSGT: Final Design and Test of a Ceramic Hot Section"; ASME Paper GT2003-38978, Published in the *Proceedings of the ASME TURBO EXPO*, Atlanta, GA, June 16–19, 2003.

[16]W. D. Carruthers, E. H. Kraft, M. Yoshida, K. Tanaka, R. Kubo, H. Terazono, and S. Tsuruzono, "Technology Development at Kyocera Corporation"; pp. 125–4 in *Ceramic Gas Turbine Component Development and Characterization, Progress in Ceramic Gas Turbine Development*, Vol. 2, Edited by M. van Roode, M. K. Ferber, and D. W. Richerson. ASME Press, New York, NY, 2003.

[17]S. M. Wiederhorn, R. F. Krause, F. Lofaj, and U. Taffner, "Creep Behavior of Improved High Temperature Silicon Nitride"; pp. 381–92 in *Key Engineering Materials*, Edited by H.-D. Kim, H.-T. Lin, M.J. Hoffmann. Trans Tech Publications, Zurich, Switzerland, 2005.

[18]M. Brito AIST, Japan, personal communication.

[19]R. Thiruvengadaswamy and R. O. Scattergood, "Biaxial Flexure Testing of Brittle Materials," *Scripta Metall. Mater.*, **25**, 2529–32 (1991).

[20]D. K. Shetty, A. R. Rosenfield, P. McGuire, B. K. Bansal, and W. H. Duckworth, "Biaxial Flexure Tests for Ceramics," *Ceram. Bull.*, **59** [12] 1193–7 (1980).

[21]G. de With and H. M. Wagemans, "Ball-on-Ring Test Revisited," *J. Am. Ceram. Soc.*, **72** [8] 1538–41 (1989).

[22]R. A. Wenglarz and K. Kouns, "Ceramic Vanes for a Model 501-K Industrial Turbine Demonstration"; ASME Paper 2000-GT-73, Published in the *Proceedings of the ASME TURBO EXPO 2000, Land, Sea, & Air*, Munich, Germany, May 8–11, 2000.

[23]M. K. Ferber, H. T. Lin, V. Parthasarathy, and R. A. Wenglarz, "Degradation of Silicon in High Pressure, Moisture Rich Environments"; ASME paper 2000-GT-661, Published in the *Proceedings of the ASME TURBO EXPO 2000, Land, Sea, & Air*, Munich, Germany, May 8–11, 2000.

[24]H. T. Lin, M. K. Ferber, W. Westphal, and F. Macri, "Evaluation of Mechanical Reliability of Silicon Nitride Vanes After Field Tests in an Industrial Gas Turbine"; ASME Paper GT2002-30629, Published in the *Proceedings of the ASME TURBO EXPO Land, Sea, & Air*, Amsterdam, The Netherlands, June 3–6, 2002.

[25]E. J. Opila, "Variation of the Oxidation Rate of SiC in Water Vapor," *J. Am. Ceram. Soc*, **82** [3] 625–36 (1999).

[26]J. K. Smialek, R. C. Robinson, E. J. Opila, D. S. Fox, and N. S. Jacobson, "SiC and Si_3N_4 Recession due to SiO_2 Scale Volatility Under Combustor Conditions," *Adv. Composite Mater.*, **8** [1] 33–45 (1999).

[27]M. K. Ferber, H. T. Lin, and J. R. Keiser, "Oxidation Behavior of Non-Oxide Ceramics in a High-Pressure, High-Temperature Steam Environment"; pp. 201–15 in *Mechanical Thermal and Environmental Testing and Performance of Ceramic Composites and Components, ASTM STP 1392*, Edited by M. G. Jenkins, E. Lara-Curzio, and S. T. Gonczy. American Society for Testing and Materials, West Conshohocken, PA, 2000.

[28]K. L. More, P. F. Tortorelli, M. K. Ferber, and J. R. Keiser, "Observations of Accelerated Silicon Carbide Recession by Oxidation at High Water-Vapor Pressures," *J. Am. Ceram. Soc.*, **83** [1] 211–3 (2000).

[29]H. T. Lin and M. K. Ferber, "Mechanical Reliability Evaluation of Silicon Nitride Ceramic Components After Exposure in Industrial Gas Turbines," *J. Eur. Ceram. Soc.*, **22**, 2789–97 (2002).

[30]H. T. Lin and M. K. Ferber, "Characterization of Mechanical Reliability of Silicon Nitride Microturbine Rotors," *Key Eng. Mater.*, **287**, 393–403 (2005). □